Journal of Medicinal Chemistry

pubs.acs.org/jmc

Article

Mitochondria-Targeted Photoactivatable Real-Time Monitoring of a Controlled Drug Delivery Platform

Neelu Singh,[⊥] Ajay Gupta,[⊥] Puja Prasad,[#] Raj Kumar Sah,[#] Arvind Singh, Sunil Kumar, Shailja Singh, Shalini Gupta, and Pijus K. Sasmal*

Cite This: https://doi.org/10.1021/acs.jmedchem.1c00956

Read Online

ACCESS | Metrics & More | Article Recommendations | Supporting Information

ABSTRACT: The current anticancer therapies are limited by their lack of controlled spatiotemporal release at the target site of action. We report a novel drug delivery platform that provides on-demand, real-time, organelle-specific drug release and monitoring upon photoactivation. The system is comprised of a model anticancer drug doxorubicin, an alkyltriphenylphosphonium moiety to target mitochondria in cancer cells, and a hydroxycinnamate photoactivatable linker that is covalently attached to the drug and mitochondria-targeting moieties such that it can be phototriggered by either UV (one-photon) or NIR (two-photon) light to form a fluorescent coumarin product and facilitate the release of drug payload. The extent of drug release is quantified by the fluorescence intensity of the coumarin formed. Further, the photoactivatable prodrug accumulates in the mitochondria and shows light-triggered temporally controlled cell death. In the future, our platform can be tuned for any biological application of interest, offering immense value in biomedicine.

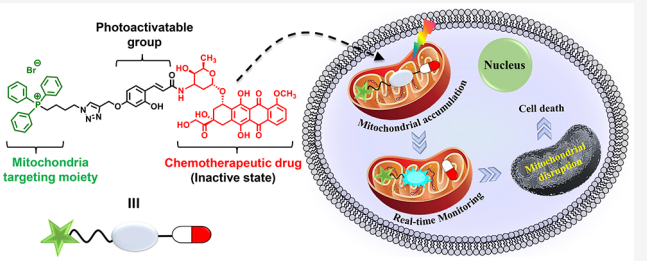

INTRODUCTION

Targeted delivery and controlled release of drugs is of enormous interest in the field of cancer. The therapeutic index of a drug is greatly enhanced if it can be delivered to a desired site of action in high amounts while being released in a controlled manner to minimize side effects.[1,2] To address the delivery problems with pharmaceuticals, various prodrug strategies have been utilized in the literature to achieve site-selective activation of prodrugs based on factors like pH,[3] redox,[4] reactive oxygen species,[5] enzymes,[6] temperature,[7] and light.[8] Among these, light-triggered drug delivery systems (DDSs) are more superior since the release of drug can be modulated by simply adjusting the wavelength, intensity, or time of exposure of light to attain high-precision spatiotemporal control over the process.[9] To date, different light-responsive DDSs have been developed using well-known photocleavable groups such as *o*-nitrobenzyl,[8a,b,10] coumarinyl,[8a,c,11] anthracenyl,[12] quinolinyl,[8a,13] *p*-hydroxyphenacyl,[8a,14] and *o*-hydroxycinnamate.[8a,15] Within these, coumarinyl-,[8c,11] *p*-hydroxyphenacyl-, and *o*-hydroxycinnamate-based systems have gained more traction due to their two-photon phototriggering capability. In the past few years, researchers have demonstrated *o*-hydroxycinnamate platforms for the uncaging of alcohols with real-time monitoring using one- and two-photon irradiation.[15c,d,g] The groups of Zhang and Wang have reported an *o*-hydroxycinnamate-based theranostic prodrug system for tumor selected controlled release of anticancer drugs triggered by hypoxia (internal stimuli) and UV-light (external stimuli).[16] The challenge, however, remains how to photorelease the therapeutic drug upon delivery to an individual organelle at a specific time to ensure its maximum utilization without dispersing the drug all over the tissue.

To this end, mitochondria-targeting DDSs have attracted considerable attention in the past few years due to the growing evidence that mitochondrial dysfunction is responsible for a wide variety of human pathological conditions such as cancer, neurodegeneration, diabetes and obesity.[17] Mitochondria are well-known to be the powerhouses in eukaryotic cells, needed for essential energy production and their survival. However, they also play a pivotal role in initiating apoptotic pathways for programmed cell death, which is regarded as the major mode of battle in cancer therapy. Therefore, a strategy based on mitochondria-targeted therapy is a promising approach for effective cancer treatment. A few recent reports in the literature specifically focus on nanomaterial-based DDSs for light-triggered drug release in mitochondria. For example, Cui et al. have demonstrated this concept using thermoresponsive liposomes with high photodynamic therapeutic efficacy in combination with photothermal effect upon near-infrared

Received: May 27, 2021

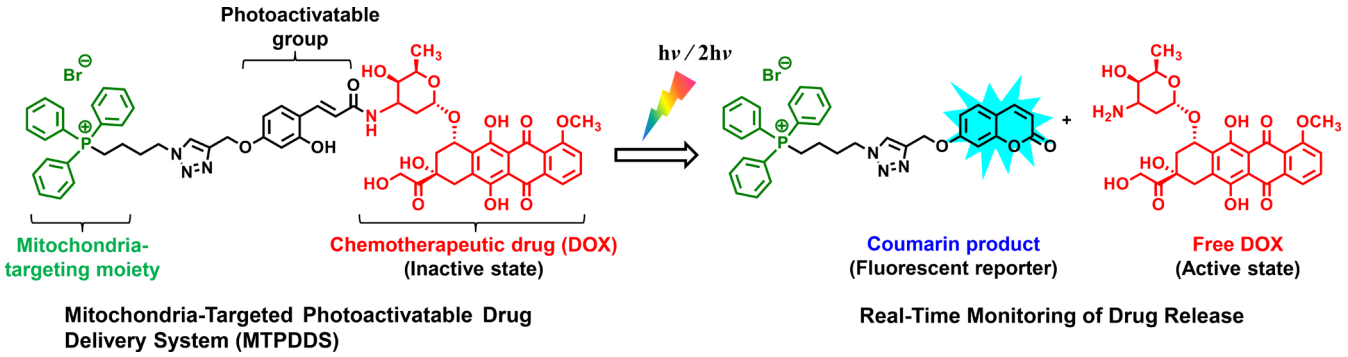

Figure 1. The *o*-hydroxycinnamate platform for targeted photoactivated drug release. A mitochondria-targeted photoactivatable drug delivery system (**MTPDDS**) that undergoes photochemical reaction upon one- or two-photon irradiation and releases a covalently bound drug along with a fluorescent coumarin coproduct in a 1:1 stoichiometric ratio.

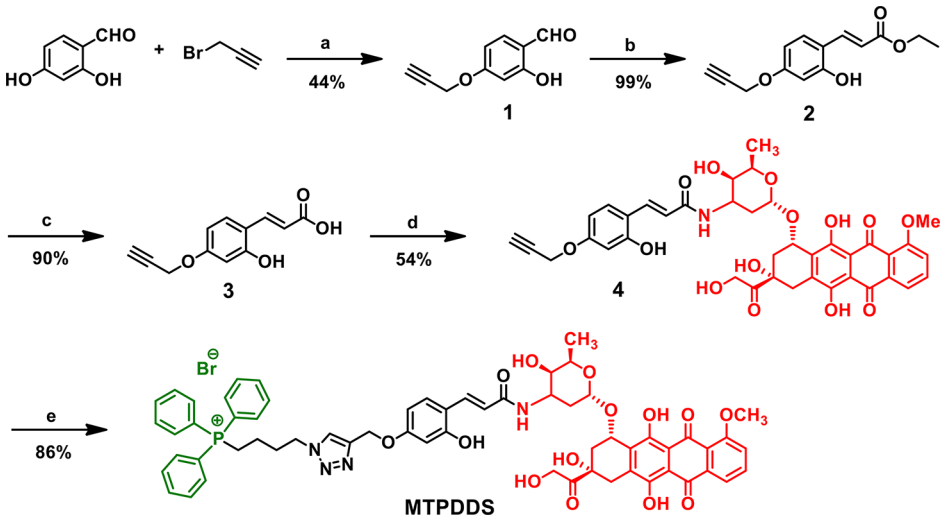

Figure 2. Schematic routes for **MTPDDS** synthesis. (a) K_2CO_3, acetone, 50 °C, 5 h; (b) $Ph_3P{=}CHCOOC_2H_5$, toluene, 60 °C, 3 h; (c) NaOH, EtOH, RT, overnight; (d) doxorubicin hydrochloride, EDC/HOBt, Et_3N, DMF, 0 °C to RT, overnight; and (e) (4-azidobutyl)-triphenylphosphonium bromide (**5**), $CuSO_4$, sodium ascorbate, THF/H_2O (10:1 v/v), RT, 6 h.

(NIR) light irradiation.[18] Qu and Ren have reported aptamer-conjugated mesoporous silica-encapsulated gold nanorods loaded with various hydrophobic therapeutic agents for mitochondria-targeted chemo-photothermal therapy.[19] In an another report, Dhar and co-workers have developed a drug delivery vehicle based on biodegradable polymer-encapsulated photosensitizer (drug) that initiates apoptosis upon light activation.[20] And to the best of our knowledge, there exists only a single report on mitochondria-targeted small-molecule photocaged rhodamine dye which allows real-time monitoring of anticancer drug.[21] However, this system too shows phototriggered drug release using green light (546 nm) which does not fall in the phototherapeutic window (650–850 nm), where the light has maximum penetration and least harmful effects on human tissues.[22]

In this paper, we have developed a mitochondria-targeted *o*-hydroxycinnamate-based UV and NIR photoactivatable DDS (**MTPDDS**) that provides full temporal-control over drug release with real-time monitoring (Figure 1). Although, UV-light activated *o*-hydroxycinnamate DDS have been reported earlier,[16] there is no analogue of such a system in the phototherapeutic window, which hinders their biomedical applications. Our **MTPDDS** has three distinct constituents: (1) a chemotherapeutic drug, (2) a targeting moiety for site-selective delivery, and (3) a photoactivatable compound chemically appended to the chemotherapeutic drug and the targeting moiety at either end to facilitate drug release upon photoirradiation. The *o*-hydroxycinnamic platform serves as a phototriggerable group that can be excited with UV- or NIR-light via two-photon excitation. In addition, a widely used alkyltriphenylphosphonium (TPP) moiety[23] is conjugated with the phototriggered compound to achieve its successful delivery to the mitochondria. The acid functionality of the photo-triggered compound is employed for caging a model anticancer drug doxorubicin (**DOX**), to demonstrate mitochondrial delivery. The nonfluorescent *o*-hydroxycinnamic amide under-goes photoinduced isomerization followed by cyclization, which facilitates the release of **DOX** together with the formation of a fluorescent coumarin coproduct in a 1:1 stoichiometric ratio (see Figure 1). The formation of this fluorescent coumarin product serves as a reporter to quantify substrate delivery and provides a much better control over drug release as and when required. This knowledge is highly desirable to obtain a quantitative drug release profile while greatly aiding in the decision making for dose administration and thereby minimizing side effects.

https://doi.org/10.1021/acs.jmedchem.1c00956
J. Med. Chem. XXXX, XXX, XXX−XXX

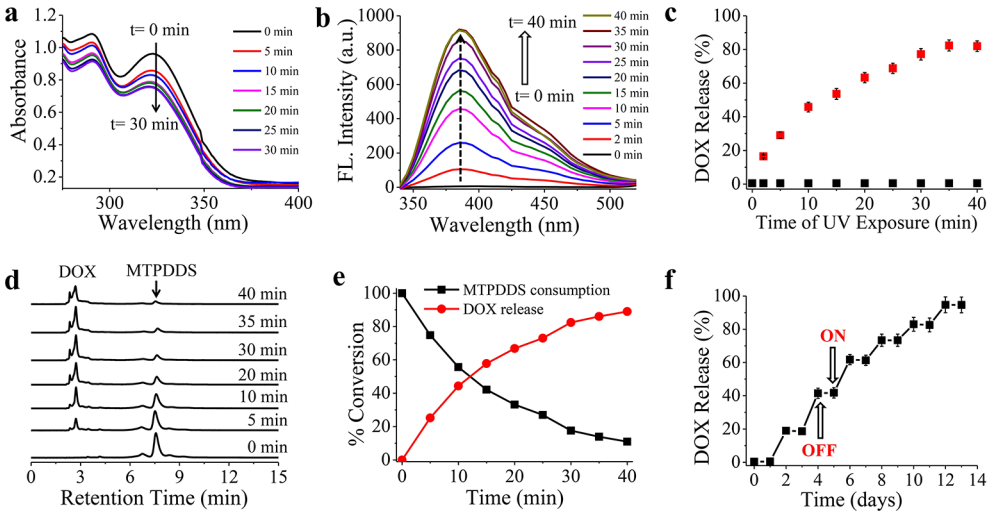

Figure 3. Phototriggered *in vitro* drug release. The **DOX** released from **MTPDDS** (50 μM) in 1:1 MeCN and phosphate buffer (100 mM, pH 7.3) monitored using UV−vis and fluorescence spectroscopy and HPLC upon photoirradiation (365 nm, 1.2 mW/cm^2) at 25 °C. (a) UV−vis spectra of **MTPDDS** recorded every 5 min of photoirradiation. (b) Time-resolved fluorescence spectra of the formed coumarin product (λ_{ex} = 325 nm) upon photoirradiation of **MTPDDS**. (c) The amount of **DOX** released from **MTPDDS** in the presence (red, solid square) and absence (black, solid square) of photolysis as a function of time. (d) HPLC chromatograms of **MTPDDS** measured at 480 nm at various photoexposure time points. (e) Kinetic plots of **MTPDDS** conversion (%) to **DOX** corresponding to the HPLC chromatograms shown in (d). (f) **DOX** (%) released under "OFF" and "ON" conditions. "OFF" and "ON" signify the switching off (48 h) and on (5 min) of the light source, respectively. Error bars signify one standard deviation (±1 SD) from three independent experiments.

RESULTS AND DISCUSSION

Design, Synthesis, and Characterization of MTPDDS. A key feature of our system relied on building a stable but phototriggerable chemical linkage between the drug and the mitochondria-targeting moiety to allow spontaneous release of the covalently bound drug upon photoirradiation (Figure 2). Realizing this strategy involved a synthetic approach wherein the phototriggerable compound 2,4-dihydroxycinnamic acid was covalently bound to the model drug **DOX**, a DNA topoisomerase II inhibitor, to release the drug in a controlled fashion. For this, the commercially available 2,4-dihydroxybenzaldehyde was used as a building block for the photoactivatable compound and reacted with propargyl bromide to isolate 4-propargyloxy-2-hydroxybenzaldehyde (**1**). The formyl group of the synthesized compound was further reacted with carboethoxymethylidenetriphenylphosphorane by the Wittig reaction to obtain the phototriggerable *o*-hydroxy-*trans*-cinnamic ester (**2**) and its subsequent hydrolysis gave *o*-hydroxy-*trans*-cinnamic acid (**3**). The carboxylic acid group of the phototriggerable compound was then used for **DOX** caging through EDC/HOBt coupling to provide a phototriggerable caged **DOX** (**4**). Finally, the propargyl group of the phototriggerable caged **DOX** was made to undergo a Click reaction with the mitochondria targeting moiety, (4-azidobutyl)triphenylphosphonium bromide (**5**), to yield **MTPDDS**. The synthesis of a reference coumarin compound for comparison is described in the Supporting Information. A model photocaged compound (**MPC**) was also synthesized by reacting phototriggered *o*-hydroxy-*trans*-cinnamic acid (**3**) with phenylethyl amine. Detailed synthetic procedures and characterization for this are also provided in the Supporting Information (Schemes S1 and S2 and Figures S1−S8).

The photophysical properties of **MTPDDS** and reference coumarin were studied in MeCN/PBS (100 mM, pH 7.3) (1:1 v/v). The **MTPDDS** showed absorption peaks at 289 nm, 323 nm and ca. 490 nm (Figure S9a). The presence of peak at ca. 490 nm suggested the successful conjugation of *o*-hydroxy-*trans*-cimmanic acid to **DOX**. Similarly, reference coumarin showed a strong absorption peak at 321 nm and an emission at 385 nm (Figure S9b). The absorption band at 323 nm in **MTPDDS** was used for photoexcitation, and the quantum yield (Φ) for reference coumarin was determined as 16.6% in MeCN/PBS using quinine sulfate (Φ = 54%) as the reference. The solid-state structure of **MPC** was also characterized by X-ray crystallography (Figure S10 and Tables S1 and S2), which confirmed *trans* conformation of the aliphatic double bond [C(10)−C(11)].

***In Vitro* Photo-Triggered Drug Release.** The release kinetics of **DOX** was evaluated by photoirradiating the **MTPDDS** solution (50 μM) using a UV lamp (365 nm, 1.2 mW/cm^2), and the drug release was monitored by absorption and emission spectroscopy, mass spectrometry and high-performance liquid chromatography (HPLC). To monitor **DOX** release by absorption spectroscopy, **MTPDDS** was exposed to UV light of 365 nm, and the absorbance spectra were recorded every 5 min of photoirradiation. The results showed that the absorbance gradually decreased with time and eventually saturated after 30 min (Figures 3a and S11a). Further, the drug release was also studied by measuring the emission spectra of the coumarin product (λ_{ex} = 325 nm) after photoexposure of **MTPDDS** at 365 nm for 2−40 min. Before irradiation, no emission of **MTPDDS** was observed at 385 nm (λ_{em} of coumarin product), suggesting that there was no formation of coumarin product. However, upon photoirradiation, the emission intensity of coumarin product gradually increased and saturated after 35 min (Figures 3b,c and S11b). In this way, the formation of fluorescent coumarin product was found to be useful for controlled and real-time monitoring of drug release. Further, the mass spectra of **MTPDDS** measured before and after photoirradiation confirmed that **MTPDDS** photochemically converted into

https://doi.org/10.1021/acs.jmedchem.1c00956
J. Med. Chem. XXXX, XXX, XXX−XXX

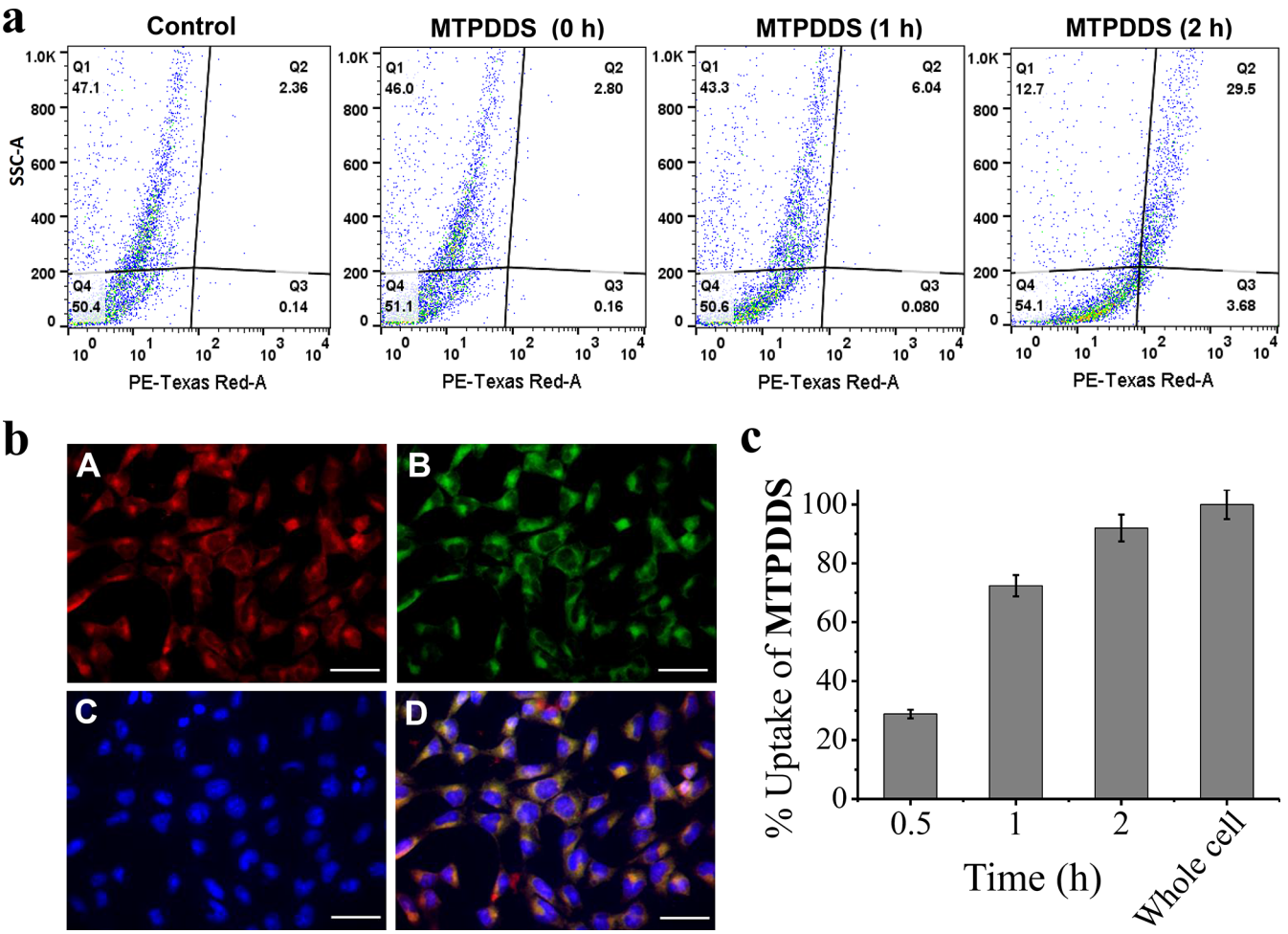

Figure 4. Cellular uptake and subcellular localization. (a) Flow cytometry dot plots of HeLa cells treated with **MTPDDS** (20 μM) for different incubation periods. The control represents untreated cells. Each data point indicates mean ±1 SD (n = 3). (b) Subcellular localization of **MTPDDS** (10 μM) in HeLa cells examined by fluorescence microscopy: (A) fluorescence image of cells treated with **MTPDDS**, (B) mitochondrial staining with Mito Tracker Green FM, (C) nuclear staining with Hoechst 33342, and (D) upon merging of images A, B, and C. Scale bar = 10 μm. (c) Percentage uptake of **MTPDDS** (20 μM) within mitochondria of HeLa cells monitored by fluorescence spectroscopy. The fluorescence intensity of cells treated with **MTPDDS** was considered as 100% which represent as a "whole cells". Error bars signify standard deviation obtained from three independent experiments.

coumarin and released **DOX** in a 1:1 molar ratio (Figures S12 and S13).

Next, we examined **DOX** release from **MTPDDS** by carefully monitoring the photochemical reaction using RP-HPLC. HPLC chromatograms were recorded before and after irradiation by monitoring the release of coumarin product and **DOX** at 325 and 480 nm, respectively. A single peak of **MTPDDS** was observed at the retention time of 7.5 min in HPLC before photoexposure. However, the intensity of this peak gradually decreased upon photoexposure with the formation of two new peaks at 6.4 and 2.7 min, corresponding to coumarin product and **DOX**, respectively (Figures 3d and S14a). Quantification of the HPLC chromatograms suggested 89% conversion of **MTPDDS** to coumarin and covalently bound drug (**DOX**) in a 1:1 stoichiometric ratio upon 40 min of photoirradiation (Figures 3e and S14b). This result was in agreement with our data obtained from absorption and emission spectroscopy. We have also examined the effect of pH in drug release profile from our prodrug (**MTPDDS**) after photoirradiation. The results show that the drug release profile does not change over a wide pH range of 4−9 (Figure S15). The prodrug also remains stable over this entire pH range. Interestingly, there was no drug release even after 30 days of incubation of **MTPDDS** in the absence of light, but the drug could subsequently be released upon photoirradiation, which established the high robustness, chemical stability, light sensitivity, and temporal behavior of our system. The mechanism of photouncaging reaction was believed to be **MTPDDS** prodrug photoisomerization from *o*-hydroxy-*trans*-cinnamic amide to *o*-hydroxy-*cis*-cinnamic amide intermediate followed by lactonization,[15d] which subsequently releases **DOX** and fluorescent coumarin coproduct in a 1:1 stoichiometric ratio (Figure S16).

To demonstrate the precise control over photoactivatable drug release in our system, we monitored the phototriggered uncaging reaction using an alternating ON/OFF switch. For this, **MTPDDS** was incubated for 24 h in the dark (OFF) and then exposed to UV light for 5 min (ON). The solution was then again incubated for 48 h in the dark (OFF) followed by exposure to UV light for 5 min (ON) and so on. This cycle was repeated six times over a period of 13 days to estimate the repeatability and trigger-induced release capability of our system. We observed a stepwise drug release only upon photoirradiation and no release in its absence (Figure 3f),

https://doi.org/10.1021/acs.jmedchem.1c00956
J. Med. Chem. XXXX, XXX, XXX−XXX

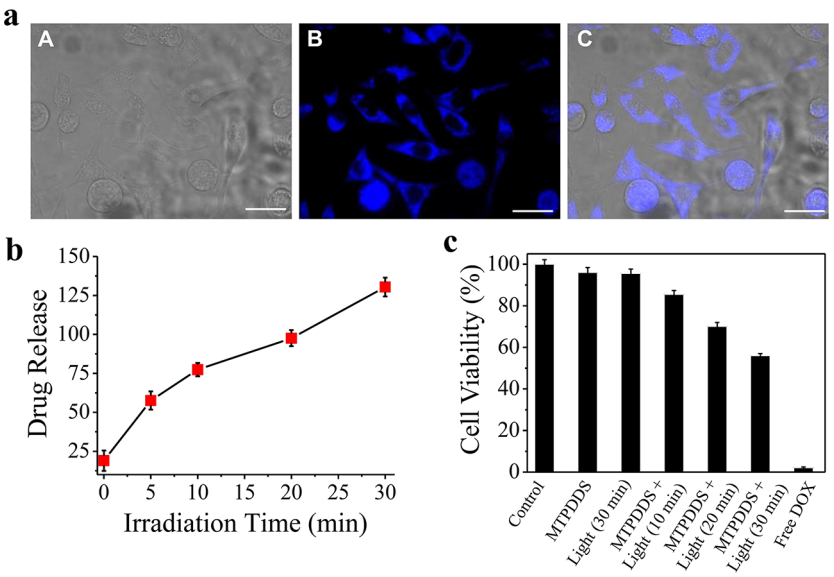

Figure 5. Light-triggered controlled drug release and photocytotoxicity. (a) Optical micrographs of HeLa cells treated with **MTPDDS** (10 μM) followed by photoirradiation at 365 nm for 10 min: (A) under bright-field, (B) using fluorescence microscopy showing formed coumarin product, and (C) after merging of images A and B. Scale bar = 10 μm. (b) Controlled drug release determined by measuring the blue fluorescence intensity of formed coumarin product using fluorometric analysis. The cells incubated with **MTPDDS** (20 μM) were irradiated with 365 nm light for different time periods. (c) MTT assay performed with HeLa cells treated with **MTPDDS** (20 μM) for 72 h to determine their viability in the absence or presence of light (365 nm, 1.2 mW/cm^2). The effect of photoirradiation was studied for varying time durations. Error bars signify standard deviation obtained from three independent experiments.

highlighting the on-demand and precise control over drug release in our system.

Cellular Uptake and Subcellular Localization. The events of phototriggered uncaging reaction encouraged us to study the uptake of **MTPDDS** in cancer cells. The uptake of any compound inside cells is greatly influenced by its lipophilicity.[24,25] Therefore, we determined the lipophilicity (log $P_{o/w}$ value) of **MTPDDS** by measuring its partition coefficient in an n-octanol/water system using the classical flask-shaking technique.[25] The value of lipophilicity was found to be 3.7, indicating the lipophilic nature of **MTPDDS**. Next, we examined the uptake of **MTPDDS** in human cervical cancer (HeLa) cells using fluorescence activated cell sorter (FACS) analysis. The uptake of **MTPDDS** increased with the incubation time from 2.8% at 0 h to 6.04% in 1 h and 29.5% in 2 h (Figure 4a). Whereas, the maximum amount of uptake of free **DOX** in HeLa cells was found to be 62% at 3 h (Figure S17). To further investigate the subcellular localization of **MTPDDS** inside HeLa cells, we performed a colocalization study with fluorescence microscopy imaging using organelle staining dyes. For this, the cells were treated with **MTPDDS**, followed by mitochondrial (Mito Tracker Green FM, 200 nM) and nuclear (Hoechst 33342, 500 nM) staining dyes (Figures 4b, S18, and S19). The imaging results revealed an overlap in the fluorescence intensity of **MTPDDS** (red) with that of Mito Tracker Green FM dye (green), making the cells appear overall yellow in color (Figures 4b(D), S18(D,E), and S19(D,E)). The extent of colocalization was also estimated using a scatter plot which clearly showed a complete overlap of the red and green signals (Figure S18(F)), confirming that our designed **MTPDDS** prodrug selectively accumulated in the mitochondria of the living HeLa cells. Furthermore, the mitochondrial uptake kinetics of **MTPDDS** was determined in HeLa cells using a mitochondria extraction kit by fluorescence spectroscopy. The maximum uptake of **MTPDDS** in mitochondria was determined to be 92% within 2 h (Figure 4c). This finding was in good agreement with the fluorescence imaging results.

UV-Light-Triggered Controlled Drug Release. In order to evaluate the drug release in cancer cells, **MTPDDS** was exposed to 365 nm light, and the formation of coumarin product was investigated by fluorescence microscopy. The appearance of blue color in the micrographs confirmed the formation of coumarin product and thus the successful release of **DOX** inside HeLa cells (Figure 5a). To further quantify these results, the cells were lysed after different durations of exposure to UV light, and the cell lysate was analyzed using fluorescence spectroscopy. The increase in blue fluorescence intensity with photoirradiation time (Figure 5b) confirmed the intracellular release of **DOX** in HeLa cells, paving the way for real-time monitoring and controlled release of drug with subcellular accuracy. To examine whether the released **DOX** from prodrug accumulated in mitochondria or diffused to other organelles, cells treated with **MTPDDS** were irradiated with 365 nm light for 15 min, and then the accumulation of **DOX** was monitored by microscopy imaging. The imaging results suggested that the released drug mostly accumulated within mitochondria even after 4 h postirradiation (Figure S20).

Evaluation of Photocytotoxicity in UV-Light. To check the efficacy of our approach for eradication of cancer cells, the activity of **MTPDDS** prodrug was evaluated in human cervical cancer (HeLa), human liver cancer (Huh-7), and human glioblastoma (LN-229) cell lines using MTT assay. For this, the cells were incubated with **MTPDDS** (20 μM) for 2 h and then exposed to UV light (365 nm, 1.2 mW/cm^2) for different time periods. The cells were then incubated for another 72 h before finally being treating with the MTT reagent. Control experiments were performed without **MTPDDS**, without irradiation or both. The results showed that **MTPDDS** in the absence of light had negligible cytotoxicity, which

https://doi.org/10.1021/acs.jmedchem.1c00956
J. Med. Chem. XXXX, XXX, XXX−XXX

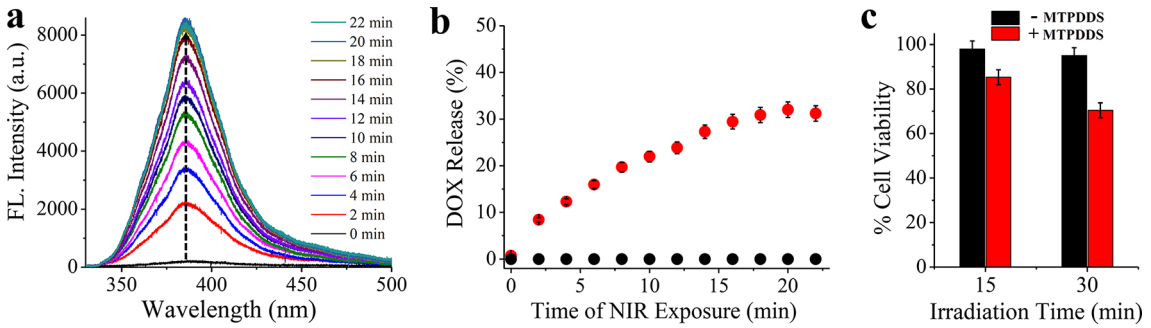

Figure 6. NIR-triggered drug release and photocytotoxicity. The **DOX** released from **MTPDDS** (50 μM) in 1:1 MeCN and phosphate buffer (100 mM, pH 7.3) upon two-photon NIR femtosecond laser light irradiation (700 nm, 50 mW) at 25 °C monitored using fluorescence spectroscopy. (a) Fluorescence spectra of the coumarin product formed (λ_{ex} = 325 nm) upon photoirradiation of **MTPDDS**. (b) **DOX** released (%) from **MTPDDS** was measured in the presence (red, solid circle) and absence (black, solid circle) of NIR-irradiation as a function of time. (c) Cell viability as determined by MTT assay in HeLa cells treated without (−) or with (+) the **MTPDDS** (20 μM) and irradiated with two-photon NIR laser (700 nm, 50 mW) for 15 and 30 min, followed by 72 h incubation. Error bars signify standard deviation obtained from three independent experiments.

suggested that **DOX** was not released from the prodrug in this case (Figures 5c and S21). Similarly, high values of cell viability were obtained with cells exposed to UV light for 30 min without any prodrug treatment. In contrast, cells treated with **MTPDDS** in the presence of UV light showed significantly reduced viability that increased as a function of light exposure; cells treated for 30 min showed more than 40% cell death. This temporal control was not possible with free **DOX** (taken at equivalent molar ratio as **MTPDDS**), which instantaneously killed all the cells (Figure 5c). We believe that the lower efficacy of **MTPDDS** is partially linked to less uptake of our prodrug in the cells due to its moderate water solubility and high lipophilicity. In order to increase the water solubility and reduce the lipophilicity of our prodrug system for any potential biological application, one could replace the lipophilic triphenylphosphonium moiety with any water-soluble mitochondria-targeting peptide or by using a less hydrophobic drug. Nevertheless, as a proof-of-concept, the system shows excellent applicability for spatiotemporally controlled drug release as per the biological application of interest.

NIR-Triggered Drug Release and Photocytotoxicity. The results of our *in vitro* drug release study further motivated us to evaluate the controlled drug release using NIR-light. The NIR-light has a far greater depth of penetration into a tissue than visible or UV-light due to its reduced absorption and scattering by water and other biological substances and least harmful effects on human tissues.[22,26] Thus, the NIR-triggered drug release system is ideal for any potential clinical application. Earlier, Jullien and co-workers showed that *o*-hydroxy-*trans*-cinnamate undergoes phototriggered cyclization reaction and transformation to coumarin and releases alcohol by two-photon NIR laser light irradiation.[15c,d] Inspired by this, we explored our phototriggered system for NIR-controlled drug release as a proof-of-concept. For this, the **MTPDDS** was exposed to NIR femtosecond laser light using two-photon excitation at 700 nm (50 mW), and the drug release was monitored by fluorescence spectroscopy (Figure 6a,b). Likewise drug release in UV-light, a temporally controlled **DOX** release was observed upon NIR-light exposure to **MTPDDS**. The result showed maximum 32% drug release after 22 min NIR-light irradiation as compared to 83% release after 40 min UV-light exposure. Although the amount of drug release is less in NIR-light as compared to the UV-light, the NIR light has various advantages over UV light in terms of clinical application. Hence, the cytotoxicity of **MTPDDS** in HeLa cells was examined with two-photon NIR-light irradiation using MTT assay (Figure 6c). Accordingly, cells were incubated with **MTPDDS** (20 μM) for 2 h and then irradiated with NIR-light (700 nm, 50 mW), followed by further incubation for 72 h before addition of MTT reagent. The cell death was found to be 29% after 30 min NIR-light irradiation with **MTPDDS**, whereas negligible cytotoxicity was observed with cells irradiated with NIR-light without treatment of **MTPDDS**. Notably, a temporally controlled cell death was also observed, wherein cell viability decreases with prodrug as a function of increase in light exposure time. The results revealed that our phototriggered system can be activated by two-photon NIR-light to control drug release and cell death, which could be thus useful in future for medicinal therapy.

CONCLUSIONS

In summary, we have developed an *o*-hydroxycinnamate-based unique drug delivery platform that provides on-demand, temporally controlled, and organelle-specific drug release with real-time monitoring by either UV (one-photon) or NIR (two-photon) light irradiation. In our designed system, we have successfully combined the mitochondria-targeting ability of alkyltriphenylphosphonium, anticancer properties of **DOX**, and photocleavable property of hydroxycinnamate moiety in-a-single platform to form **MTPDDS** that releases drug and showed spatiotemporally controlled cancer cell death upon photoirradiation. The phototriggered isomerization of **MTPDDS** led to the formation of fluorescent coumarin and **DOX** products in a 1:1 molar ratio. The formation of fluorescent coumarin product serves as a reporter to quantify drug release. The drug was precisely released only in the presence of light, which demonstrated its chemical stability and robustness. The light-mediated drug release was also directly proportional to cell death, and no cell death was seen in the absence of light, suggesting the highly specific nature of our DDS. The site-selective accumulation of the phototriggered prodrug in the mitochondria was examined by fluorescence microscopy. In **MTPDDS**, the imaging of released coumarin product was performed in the UV region, since it has an emission band at 385 nm. However, the emission of the coumarin reporter can be shifted to higher wavelengths for *in vivo* imaging applications by an appropriate substitution on the aromatic ring or extending the π-conjugation in the aromatic moiety of photocactivatable linker. The salient features of our designed system are truly "first-in-class", and its versatile design

https://doi.org/10.1021/acs.jmedchem.1c00956
J. Med. Chem. XXXX, XXX, XXX−XXX

could be adapted in the future for any desired biomedical application by simply replacing the drug (e.g., anticancer drugs, anti-inflammatories, steroids) and targeting group (e.g., cancer-cell targeting, organelle targeting, receptor-binding peptides, etc.) to control drug-dosing, reduce chemotherapeutic side effects, and overcome drug resistance.

EXPERIMENTAL SECTION

Materials. Solvents were distilled under nitrogen from calcium hydride (CH_2Cl_2), magnesium chips (MeOH), or sodium/benzophenone (THF). Toluene, MeCN, DMF, and DMSO were used as HPLC grade without further drying. The 2,4-dihydroxybenzaldehyde, propargyl bromide, potassium carbonate, carboethoxymethylidenetriphenylphosphorane, (4-bromobutyl)triphenylphosphonium bromide, 7-hydroxycoumarin, sodium phosphate dibasic, and sodium phosphate monobasic were purchased from Alfa-Aesar. Doxorubicin hydrochloride and triethylamine (Et_3N) were obtained from Sigma-Aldrich, and 1-ethyl-3-(3-dimethylaminopropyl)carbodiimide (EDC) and 1-hydroxybenzotriazole hydrate (HOBt) were sourced from SRL. Sodium hydroxide, sodium azide, copper sulfate, sodium ascorbate, and 2-phenylethyl amine were purchased from Central Drug House (CDH). Trypsin, Dulbecco's modified Eagle medium (DMEM), fetal bovine serum (FBS), 3-(4, 5-dimethylthiazol-2-yl)-2, 5-diphenyltetrazolium bromide (MTT), Dulbecco's phosphate-buffered saline (PBS), penicillin streptomycin solution (pen-strep), and 24-well plates were procured from Thermo Fischer Scientific. Mito Tracker Green FM and Hoechst 33342 were sourced from Invitrogen. Mitochondria extraction kit was purchased from Sigma-Aldrich (catalog: MITOISO2). Thin-layer chromatography (TLC) was sourced from Merck, Germany. UV lamp (Spectroline, ENF-260C/FE, 6 W/365 nm short/long wave UV lamp) was procured from Sigma-Aldrich. The purity of the compounds **1**−**5**, reference coumarin, and MPC were found to be ≥95% by NMR and high-resolution mass spectra, while the purity of final compound (**MTPDDS**) utilized for biological evaluation was determined to be ≥95% by NMR, high-resolution mass spectra and RP-HPLC.

Synthesis and Characterization. *Compound 1.* 2,4-Dihydroxybenzaldehyde (500 mg, 3.62 mmol, 1 equiv) and K_2CO_3 (500 mg, 3.62 mmol, 1 equiv) were suspended in 6 mL of acetone, and the mixture was stirred at room temperature for 20 min under argon atmosphere. Propargyl bromide (411 μL, 5.43 mmol, 1.5 equiv) was added dropwise to the above reaction mixture and then heated at 50 °C for 5 h. The progress of the reaction was monitored by TLC analysis using DCM/hexane (1:1). After completion of reaction, acetone was evaporated on a rotary evaporator, and the resulting residue was taken in DCM (30 mL), which was washed with distilled water (3 × 25 mL) and brine (25 mL). The organic layer was then dried over anhydrous $MgSO_4$, filtered, and evaporated to dryness under reduced pressure. The resulting crude product was then purified by silica gel column chromatography using DCM/hexane (1:1) as the eluent to obtain the product as an off-white solid (282 mg, 44%).

^{1}H NMR (500 MHz, $CDCl_3$): δ (ppm) 11.46 (s, 1H), 9.74 (s, 1H), 7.46 (d, J = 8.7 Hz, 1H), 6.61 (dd, J = 8.7, 2.3 Hz, 1H), 6.53 (d, J = 2.3 Hz, 1H), 4.74 (d, J = 2.4 Hz, 2H), 2.58 (t, J = 2.4 Hz, 1H). ^{13}C NMR (125 MHz, $CDCl_3$): δ (ppm) 194.58, 164.54, 164.26, 135.34, 115.71, 108.69, 101.85, 77.30, 76.79, 56.08. IR (ATR) ν (cm^{-1}): 3238 m (≡C−H), 2922 w, 2851 w (aldehyde C−H), 2129 m (C≡C), 1633 sh, 1382 m, 1286 s, 1215 s, 1186 s, 835 m, 742 m, 642 m. ESI-MS (m/z): calculated 177.0552 $[M + H]^+$, found 177.0583.

Compound 2. A mixture of compound **1** (300 mg, 1.70 mmol, 1 equiv) and carboethoxymethylidenetriphenylphosphorane (890 mg, 2.55 mmol, 1.5 equiv) in 2.7 mL of dry toluene was heated at 60 °C under argon atmosphere in dark for 3 h. Then the reaction mixture was allowed to cool to room temperature, and subsequently toluene was evaporated under reduced pressure. The obtained crude product was purified by silica gel column chromatography using hexane/EtOAc (1:1) to afford the product as light yellow crystalline solid (415 mg, 99%).

^{1}H NMR (500 MHz, acetone-d_6): δ (ppm) 9.23 (s, 1H), 7.89 (d, J = 16.1 Hz, 1H), 7.53 (d, J = 8.5 Hz, 1H), 6.55 (m, 2H), 6.46 (d, J = 16.1 Hz, 1H), 4.75 (d, J = 2.4 Hz, 2H), 4.15 (q, J = 7.1 Hz, 2H), 3.09 (t, J = 2.4 Hz, 1H), 1.24 (t, J = 7.1 Hz, 3H). ^{13}C NMR (125 MHz, acetone-d_6): δ (ppm) 166.96, 160.54, 157.85, 139.55, 130.17, 115.65, 115.39, 107.00, 102.39, 78.50, 76.45, 59.50, 55.47, 13.81. IR (ATR) ν (cm^{-1}): 3319 br, 3265 m (≡C−H), 2127 (C≡C) w, 1683 s (C═O), 1612 m, 1274 m, 1184 m, 977 m, 856 w, 797 w. ESI-MS (m/z): calculated 247.0970 $[M + H]^+$, found 247.1016.

Compound 3. Compound **2** (200 mg, 0.81 mmol, 1 equiv) was dissolved in 10 mL of EtOH and cooled to 0 °C. To this chilled solution, 2.0 M NaOH (4.7 mL) was added dropwise, and then the reaction was allowed to stir at room temperature in the dark for overnight. Then the reaction was cooled to 0 °C and acidified with 1.0 M HCl to keep pH 1−3. Next, the solvent was removed on a rotary evaporator, and the resulting aqueous phase was extracted with EtOAc (3 × 25 mL). The combined organic phase was further washed with brine (25 mL), dried over anhydrous $MgSO_4$, filtered, and evaporated to achieve the product as white solid (160 mg, 90%).

^{1}H NMR (500 MHz, DMSO-d_6): δ (ppm) 12.05 (s, 1H), 10.35 (s, 1H), 7.73 (d, J = 16.1 Hz, 1H), 7.53 (d, J = 8.5 Hz, 1H), 6.49 (m, 2H), 6.38 (d, J = 16.1 Hz, 1H), 4.77 (d, J = 2.1 Hz, 1H), 3.62 (s, 1H). ^{13}C NMR (125 MHz, DMSO-d_6): δ (ppm) 168.80, 160.33, 158.44, 139.88, 130.46, 116.29, 115.29, 107.06, 102.60, 79.45, 78.95, 55.90. IR (ATR) ν (cm^{-1}): 3279 w (≡C−H), 3205 br, 2851 w, 2135 w (C≡C) m, 1664 m, 1431 m, 1269 m, 1186 m, 982 s, 872 m, 651 w. ESI-MS (m/z): calculated 219.0657 $[M + H]^+$, found 219.0661.

Compound 4. Compound **3** (5 mg, 0.023 mmol, 1 equiv) was dissolved in 250 μL of DMF and cooled to 0 °C. To this cooled solution, EDC (13 mg, 0.068 mmol, 3 equiv) was added and stirred for 10−15 min at 0 °C. Then, HOBt (7 mg, 0.046 mmol, 2 equiv) was added and allowed to stir at 0 °C for another 10−15 min. To the above mixture, Et_3N (6.3 μL, 0.046 mmol, 2 equiv) and DOX (14.6 mg, 0.025 mmol, 1.1 equiv) were added and allowed to stir at 0 °C for additional 2 h and then at room temperature for overnight in dark under argon atmosphere. Then the reaction was diluted with saturated $NaHCO_3$ solution (30 mL) and extracted with EtOAc (5 × 30 mL). The combined organic phase was dried over anhydrous $MgSO_4$, filtered, and evaporated on a rotary evaporator. The resulting crude material was then purified by silica gel column chromatography using DCM/MeOH (10:1) as an eluent to obtain the product as red solid (9.3 mg, 54%).

^{1}H NMR (500 MHz, DMSO-d_6): δ (ppm) 14.05 (s, 1H), 13.24 (s, 1H), 10.16 (s, 1H), 7.90 (d, J = 4.5 Hz, 2H), 7.70 (d, J = 8.3 Hz, 1H), 7.63 (t, J = 5 Hz, 1H), 7.49 (d, J = 15.8 Hz, 1H), 7.33 (d, J = 8.3 Hz, 1H), 6.61 (d, J = 15.8 Hz, 1H), 6.45 (m, 2H), 5.51 (s, 1H), 5.24 (d, J = 2.5 Hz, 1H), 4.94 (t, J = 4.0 Hz,, 1H), 4.89 (t, J = 5.9 Hz, 1H), 4.85 (d, J = 6 Hz, 1H), 4.73 (d, J = 2.1 Hz, 2H), 4.59 (d, J = 5.8 Hz, 2H), 4.20 (q, J = 6.4 Hz, 1H), 4.09 (m, 1H), 3.97 (s, 3H), 3.60 (t, J = 2.2 Hz, 1H), 2.97 (m, 2H), 2.22 (d, J = 13.9, 1H), 2.12 (m, 1H), 1.98 (m, 1H), 1.89 (td, J = 12.9, 3.4 Hz, 1H), 1.47 (dd, J = 12.1, 3.9 Hz, 1H), 1.13 (d, J = 6.5 Hz, 3H). ^{13}C NMR (125 MHz, DMSO-d_6): δ (ppm) 214.29, 187.01, 186.91, 165.50, 161.25, 159.48, 157.81, 156.59, 154.98, 136.67, 136.03, 135.13, 134.56, 134.30, 129.40, 120.48, 120.17, 119.45, 116.08, 111.25, 111.12, 106.81, 102.67, 100.89, 79.57, 78.86, 75.45, 70.46, 68.63, 67.20, 64.16, 57.04, 55.83, 45.51, 40.88, 37.16, 22.58, 17.53, 14.42. IR (ATR) ν (cm^{-1}): 3356 br, 2920 sh, 1724 w (C═O), 1608 m (C═C), 1578 m (N−H), 1283 m (C−O−C), 1080 w (C−O), 977 m, 873 w. ESI-MS (m/z): calculated 782.1851 $[M + K]^+$, found 782.1802.

(4-Azidobutyl)triphenylphosphonium Bromide (5). (4-Bromobutyl)triphenylphosphonium bromide (500 mg, 1.04 mmol, 1 equiv) and sodium azide (204 mg, 3.13 mmol, 3 equiv) were suspended in 10 mL of DMF and heated at 85 °C under an argon atmosphere for overnight. Then the reaction was allowed to cool to room temperature, diluted with DCM (40 mL), and extracted with distilled water (3 × 30 mL). The organic phase was dried over anhydrous $MgSO_4$, filtered, and evaporated on a rotary evaporator to afford the product as reddish-orange oil (398 mg, 87%).

https://doi.org/10.1021/acs.jmedchem.1c00956
J. Med. Chem. XXXX, XXX, XXX−XXX

^{1}H NMR (500 MHz, $CDCl_3$): δ (ppm) 7.79 (m, 9H), 7.67 (m, 6H), 3.84 (m, 2H), 3.40 (t, J = 6.1 Hz, 2H), 1.96 (m, 2H), 1.69 (m, 2H).

Mitochondria-Targeted Photoactivatable Drug Delivery System (MTPDDS). Compounds **4** (12 mg, 0.016 mmol, 1 equiv) and **5** (14.2 mg, 0.032 mmol, 2 equiv) were suspended in 680 μL of THF and stirred at room temperature. To this, $CuSO_4{\cdot}5H_2O$ (0.8 mg, 0.0032 mmol, 0.2 equiv) and sodium ascorbate (1.6 mg, 0.008 mmol, 0.5 equiv) in deionized water (68 μL) were added, and the reaction was allowed to stir at room temperature in dark under argon atmosphere for 6 h. The course of reaction was monitored by TLC analysis using DCM/MeOH (10:1). After completion of the reaction, the solvent was removed under reduced pressure, and the resulting crude material was washed with DCM to remove the unreacted azide. Finally, the precipitate was then washed with 1:1 $CHCl_3$/MeOH to remove the $CuSO_4{\cdot}5H_2O$ and sodium ascorbate to yield product as dark red solid (16.4 mg, 86%).

^{1}H NMR (500 MHz, DMSO-d_6): δ (ppm) 14.03 (s, 1H), 13.26 (s, 1H), 10.26 (s, 1H), 8.17 (s, 1H), 7.88 (m, 6H), 7.78 (m, 15H), 7.63 (m, 1H), 7.49 (d, J = 15.7 Hz, 1H), 7.32 (d, J = 8.5 Hz, 1H), 6.61 (d, J = 15.8 Hz, 1H), 6.52 (m, 2H), 5.51 (s, 1H), 5.24 (s, 1H), 5.05 (s, 2H), 4.94 (s, 1H), 4.59 (s, 2H), 4.44 (m, 2H), 4.21 (m, 1H), 4.09 (m, 1H), 3.96 (s, 3H), 3.49 (s, 1H), 2.97 (q, J = 18.0 Hz, 2H), 2.23 (d, J = 13.6 Hz, 1H), 2.12 (m, 1H), 2.01 (m, 2H), 1.89 (t, J = 11.2 Hz, 1H), 1.49 (m,, 3H), 1.34 (d, J = 9.4 Hz, 1H), 1.23 (s, 2H), 1.14 (d, J = 6.1 Hz, 3H). ^{13}C NMR (125 MHz, DMSO-d_6): δ (ppm) 213.91, 186.56, 186.48, 165.09, 160.80, 159.81, 157.57, 156.16, 154.54, 142.43, 134.98, 133.62, 133.54, 130.33, 130.23, 129.04, 124.61,120.01, 119.76, 119.51, 119.01, 118.78, 118.66, 118.09, 117.90, 115.33, 110.80, 110.66, 106.09, 102.18, 100.47, 75.00, 70.04, 68.21, 66.76, 63.73, 60.97, 56.60, 49.83, 49.43, 48.14, 45.09, 40.43, 36.71, 32.11, 31.57, 30.29, 30.15, 29.87, 29.03, 25.15, 22.12, 19.79, 19.38, 18.78, 17.10.. IR (ATR) ν (cm^{-1}): 3290 br, 2922 m, 1724 w (C═O), 1653 m, 1604 m (C═C), 1587 m (N−H), 1282 m (C−O−C), 1018 m (C−O), 981 m, 723 w. ESI-MS (m/z): calculated 1103.3839 $[M]^+$, found 1103.2312.

Drug Release Study by UV−vis Spectroscopy. The kinetics of drug release was monitored upon photoexposure of **MTPDDS** by UV−vis spectroscopy. **MTPDDS** (50 μM) was dissolved in 1:1 MeCN/PBS and exposed to the light (365 nm, 1.2 mW/cm^2) for 0−30 min. The **MTPDDS** solution (50 μM) was taken in a quartz cuvette and exposed to light at a distance of 2 cm from the UV lamp. Each time, the solution was exposed to the light for 5 min followed by incubation for 30 min at 25 °C before recording the absorption spectrum.

Drug Release Study by Fluorescence Spectroscopy. The drug release was also studied upon photoexposure (365 nm, 1.2 mW/cm^2) of the **MTPDDS** solution (50 μM) in 1:1 MeCN/PBS via fluorescence spectroscopy. The exposure of sample to light was performed at a distance of 2 cm from the light source. The fluorescence spectra of **MTPDDS** were measured after several durations of photoirradiation (t = 2, 3, 5, 10, 15, 20, 25, 30, 35, and 40 min) followed by incubation at 25 °C for 1 h after each photoirradiation event. The drug release from **MTPDDS** was monitored by measuring the emission intensity of coumarin product (λ_{ex} = 325 nm and λ_{em} = 385 nm). For the dark control experiment, a similar procedure was followed without exposure of **MTPDDS** to UV light.

Drug Release Study by Mass Spectrometry. The drug release study was also characterized using mass spectrometry by recording the mass spectra of **MTPDDS** (50 μM) in 1:1 MeCN/PBS before and after photoexposure. The solution of **MTPDDS** was exposed to UV light (365 nm, 1.2 mW/cm^2) for 30 min, followed by incubation for 3 h at 25 °C before recording the mass spectra.

Drug Release Study by HPLC. The time-dependent drug release study was also performed using HPLC. The **MTPDDS** solution (50 μM) in 1:1 MeCN/PBS (100 mM, pH 7.3) was taken in a fluorescence quartz cuvette and exposed to UV light (365 nm, 1.2 mW/cm^2) at a distance of 2 cm from the light source. Each time, the **MTPDDS** solution was exposed to UV light for 5 min and then incubated at 25 °C for 1 h. An aliquot (10 μL) was taken from the **MTPDDS** solution after each photoirradiation event and analyzed by RP-HPLC using MeCN/water (1:1), both containing 0.1% TFA in the mobile phase, at a flow rate of 1.0 mL/min. The chromatograms were analyzed at 325 and 480 nm. The relative percentage of conversion of **MTPDDS** to the coumarin product and **DOX** was determined by comparing their relative HPLC peak areas at each time point.

Cell Culture. Human cervical cancer (HeLa), human liver cancer (Huh-7), and human glioblastoma (LN-229) cells were procured from the National Center for Cell Science (NCCS) Pune. The cells were cultured in high-glucose DMEM containing 10% FBS and 1% penicillin-streptomycin at 37 °C in a 5% CO_2 humidified incubator. When the cells reached 90% confluency, they were trypsinized, centrifuged, and redispersed in complete medium. The cells were seeded in 96-well cell culture plates at a density of 9000 cells/well or in glass well 35 mm μ-dish at a density of 2 × 10^5 cells/dish and cultured for 24 h at 37 °C in 5% CO_2 incubator.

Cellular Uptake. HeLa cells were seeded in 24-well plates at a density of 5000 cells/well. The cells were washed twice in PBS and incubated with 20 μM of **MTPDDS** solution (prepared in complete cultured media containing 1% DMSO) for 0, 1, and 2 h at 37 °C. Following incubation, the cells were washed twice with PBS followed by trypsinization and resuspended in 500 μL of Hanks' balanced salt solution (HBSS). Then the red fluorescence of **MTPDDS** in HeLa cells was recorded using a flow cytometry (FACS-LSR Fortessa; BD Biosciences, U.S.A.). Approximately, 5000 cells were counted for each sample. BD FACS-DIVA Software was used to acquire the cells for each measurement. Data were analyzed using FlowJo software (Tree Star).

Subcellular Localization. The localization of **MTPDDS** inside cells was determined by fluorescence microscopy. For this, colocalization experiments were performed using organelle staining dyes. HeLa cells were seeded in 35 mm glass bottom plates μ-slides (iBidi, Germany) at a density of 2 × 10^5 cells 1 day prior to the experiments. The cells were treated with 10 μM of **MTPDDS** for 90 min in DMEM complete media. Mito Tracker Green FM (200 nM) and Hoechst 33342 (500 nM) dyes were added in the last 30 min of incubation. The media was then removed, and the cells were washed thoroughly with PBS (4 × 1 mL) before performing microscopy imaging. Images were obtained using an inverted fluorescence microscope (Olympus IX70, Tokyo, Japan) equipped with a digital camera (DP71, Olympus). **MTPDDS** fluorescence was analyzed with TRITC filter set ($\lambda_{ex}/\lambda_{em}$ = 520/596 nm). Hoechst fluorescence was analyzed with DAPI filter ($\lambda_{ex}/\lambda_{em}$ = 350/460 nm), and Mito Tracker Green fluorescence was analyzed with FITC filter set ($\lambda_{ex}/\lambda_{em}$ = 485/525 nm). The extent of colocalization was calculated by scatter plot using Mander's overlap coefficient and Pearson's correlation coefficient (PCC).

Mitochondrial Uptake Kinetics. The mitochondrial uptake of **MTPDDS** in HeLa cells was examined by fluorescence spectroscopy. For this, 4 × 10^8 cells were treated with the **MTPDDS** (20 μM) and then incubated for different time periods (0.5 h, 1 and 2 h), followed by extraction of mitochondria using a mitochondria extraction kit (Sigma-Aldrich, catalog: MITOISO2). The uptake of **MTPDDS** in mitochondria was determined by monitoring its intensity (λ_{ex} = 480 nm, λ_{em} = 590 nm) by fluorescence spectroscopy using a SpectraMax i3x microtiter plate reader (Molecular Devices LLC, USA). The fluorescence intensity of cells treated with **MTPDDS** was considered as 100%, which represents as a "whole cells".

Controlled Drug Release. The intracellular release of **DOX** was determined by measuring the intracellular fluorescence intensity of the formed coumarin product upon photoexposure of **MTPDDS**. Briefly, cells were plated in a 96-well culture plate at a density of 2 × 10^4 cells/well. The cells were then treated with **MTPDDS** (20 μM) and incubated at 37 °C for 2 h in the dark. After 2 h, the media was removed, and cells were washed with cold PBS (2 × 1 mL), followed by irradiation with UV light (365 nm, 1.2 mW/cm^2) for 5, 10, 20, and 30 min and again incubated at 37 °C for 2 h. The cells were lysed using 200 μL of lysis buffer (50 mM Tris-HCL, 150 mM NaCl, 0.1%

https://doi.org/10.1021/acs.jmedchem.1c00956
J. Med. Chem. XXXX, XXX, XXX−XXX

NP40, 0.1% SDS, 0.1% sodium deoxycholate, 1% Triton X-100), and the release of **DOX** was determined by measuring the blue fluorescence intensity of the formed coumarin product (λ_{ex} = 325 nm, λ_{em} = 385 nm) in the cell lysate by fluorometric analysis with Varioskan LUX Multimode Microplate Reader (Thermo Fisher Scientific).

Photocytotoxicity Assay in UV-Light. *In vitro* photocytotoxicity was assessed by MTT assays. A 40 μM stock solution of **MTPDDS** was prepared in a complete cultured media containing 1% DMSO. For the cytotoxicity assay, cells were cultured at a concentration of 9000 cells/well in 96-well cell culture plates with DMEM (100 μL) and incubated at 37 °C for 24 h. Then, the media from 96-well cell cultured plates were removed and replaced with 100 μL of fresh medium. To this, 100 μL of **MTPDDS** (40 μM) stock solution was added to reach a final **MTPDDS** concentration of 20 μM in 200 μL total volume. The cells were incubated with **MTPDDS** for 2 h in a CO_2 incubator in the dark, and then the media were removed from the cultured plates and replaced with 200 μL of fresh medium. Next, the cells were irradiated with or without UV light (365 nm, 1.2 mW/cm^2) for different time periods (10, 20, and 30 min), followed by further incubation in the dark for 72 h. Subsequently, the cells were washed with PBS followed by the addition of 100 μL of fresh cultured media and 20 μL of MTT solution (5 mg/mL in PBS) to each well and incubated for 2 h. The media was then discarded, and 100 μL of DMSO was added to each well to dissolve the formazan crystals formed by the living cells. The cell viability was determined by measuring absorbance at 550 nm using SpectraMax i3x microtiter plate reader (Molecular Devices LLC, USA).

NIR-Triggered Drug Release. The two-photon irradiation experiments were performed with femtosecond (fs) pulses (pulse width ~100 fs) centered at 700 nm (average power ~50 mW). The source is an optical parametric amplifier operating at 700 nm and pumped by a Ti-sapphire mode-locked regenerative femtosecond amplifier at 800 nm (1 kHz, 35 fs, Astrella, Coherent). The **MTPDDS** (50 μM) solution was irradiated for 2 min before recording fluorescence spectra every time. While irradiating the sample, we ensured maximum exposure of the sample with the laser light by making light pass through the solution from the top. Irradiation with 700 nm laser light ensured two-photon absorption in the sample. For fluorescence measurements separately, 1 mW from a continuous wave (CW) He-CD laser at 325 nm (KIMMON, Japan) was used for excitation. The fluorescence was collected using a lens and sent to a spectrometer (iHR550, Horiba Jobin Yvon, USA) for recording the spectra.

Photocytotoxicity Assay in NIR-Light. The experimental protocol was similar to photocytotoxicity assay in UV-light with slight modification. Briefly, the cultured cells (9000 cells/well) in 96-well plates containing DMEM (100 μL) were treated with 100 μL of **MTPDDS** (40 μM) stock solution to reach a final **MTPDDS** concentration of 20 μM in 200 μL total volume. The cells were incubated with **MTPDDS** for 2 h in a CO_2 incubator in the dark, and then the media were removed from the cultured plates and replaced with 200 μL of PBS. Subsequently, the cells were irradiated with or without NIR femtosecond laser light using two-photon excitation at 700 nm (50 mW) for 15 and 30 min. After photoexposure, PBS was removed and replaced with 200 μL of DMEM and further incubated for 72 h in dark. Next, the cells were washed with PBS, followed by addition of 200 μL of fresh cultured media and 20 μL of MTT solution (5 mg/mL in PBS) to each well and incubated for 2 h. The media was then discarded, and 200 μL of DMSO was added to each well to dissolve the formazan crystals formed by the living cells. The cell viability was determined by measuring absorbance at 550 nm.

■ ASSOCIATED CONTENT

Supporting Information

The Supporting Information is available free of charge at https://pubs.acs.org/doi/10.1021/acs.jmedchem.1c00956.

Instruments and methods, synthetic procedures for the compounds not described in the main paper, all relevant experimental procedures, crystallographic structure determination, crystallographic data tables, ^{1}H and ^{13}C NMR spectra for all compounds, absorption and emission spectra, ESI-MS and HPLC chromatograms of the **MTPDDS** before and after photoirradiation, effect of pH in drug release profile from **MTPDDS**, proposed mechanism of photoinduced drug release from **MTPDDS**, uptake of **DOX**, subcellular localization of **MTPDDS**, and cell viability assay plots (PDF)

MPC (CIF)

Molecular formula strings (CSV)

Accession Codes

CCDC 2058227 contains the supplementary crystallographic data for this paper. The data can be obtained free of charge via www.ccdc.cam.ac.uk/data_request/cif, or by emailing data_request@ccdc.cam.ac.uk, or by contacting The Cambridge Crystallographic Data Centre, 12 Union Road, Cambridge CB2 1EZ, UK; fax: + 44 1223 336033.

■ AUTHOR INFORMATION

Corresponding Author

Pijus K. Sasmal − *School of Physical Sciences, Jawaharlal Nehru University, New Delhi 110067, India;* orcid.org/0000-0002-2301-1269; Email: pijus@mail.jnu.ac.in

Authors

Neelu Singh − *School of Physical Sciences, Jawaharlal Nehru University, New Delhi 110067, India*

Ajay Gupta − *School of Physical Sciences, Jawaharlal Nehru University, New Delhi 110067, India*

Puja Prasad − *Department of Chemical Engineering, Indian Institute of Technology Delhi, New Delhi 110016, India*

Raj Kumar Sah − *Special Centre for Molecular Medicine, Jawaharlal Nehru University, New Delhi 110067, India*

Arvind Singh − *Department of Physics, Indian Institute of Technology Delhi, New Delhi 110016, India;* orcid.org/0000-0001-6911-1428

Sunil Kumar − *Department of Physics, Indian Institute of Technology Delhi, New Delhi 110016, India;* orcid.org/0000-0002-1065-9883

Shailja Singh − *Special Centre for Molecular Medicine, Jawaharlal Nehru University, New Delhi 110067, India;* orcid.org/0000-0001-5286-6605

Shalini Gupta − *Department of Chemical Engineering, Indian Institute of Technology Delhi, New Delhi 110016, India;* orcid.org/0000-0003-1382-0254

Complete contact information is available at: https://pubs.acs.org/10.1021/acs.jmedchem.1c00956

Author Contributions

[⊥]These authors contributed equally to this work as first authors.

Author Contributions

[#]These authors contributed equally to this work as second authors.

Notes

The authors declare no competing financial interest.

■ ACKNOWLEDGMENTS

P.K.S. acknowledges MHRD-STARS (project code: MoE-STARS/STARS-1/374) and UPE-II (project no. 256) for financial support. P.K.S. also acknowledges UGC (no. F.30-

351/2017(BSR)) for partial financial assistance. S.G. acknowledges DST Nanomission (SR/NM/NT-1049/2016) and IMPRINT grant (IMP/2018/000236/HT). S.S. acknowledges IYBA and National Bioscientist award from DBT for the funding support. We thank DST-FIST for Single Crystal X-ray Diffraction facility in SPS, JNU and AIRF, JNU for the instrumentation facilities. N.S. gratefully acknowledges the SERB, DST, for financial support as a JRF. A.G. acknowledges MHRD-STARS for a fellowship. P.P. thanks CSIR for the SRA position (pool no. 9031-A). R.K.S. acknowledges CSIR-UGC for fellowship. We thank Dr. D. Das and Ms. L. Negi, SPS, JNU, for help with the X-ray data collection and for solving crystal structure of **MPC**.

■ ABBREVIATIONS USED

UV, ultraviolet; NIR, near-infrared; DDS, drug delivery system; MTPDDS, mitochondria-targeted photoactivatable drug delivery system; TPP, triphenylphosphonium; DOX, doxorubicin; EDC, 1-ethyl-3-(3-dimethylaminopropyl)-carbodiimide; HOBt, hydroxybenzotriazole; MPC, model photocaged compound; PBS, phosphate-buffered saline; RP-HPLC, reversed-phase high-performance liquid chromatography; TLC, thin-layer chromatography; NMR, nuclear magnetic resonance; ESI-MS, electrospray ionization mass spectra; FT-IR, Fourier transform-infrared; UV−vis, ultraviolet−visible; HeLa, human cervical cancer; Huh-7, human liver cancer; LN-229, human glioblastoma; MTT, 3-(4,5-dimethylthiazol-2-yl)-2,5-diphenyltetrazolium bromide; DCM, dichloromethane; MeOH, methanol; THF, tetrahydrofuran; DMF, dimethylformamide; DMSO, dimethyl sulfoxide; Et_3N, triethylamine; MeCN, acetonitrile; EtOAc, ethyl acetate; EtOH, ethanol; RT, room temperature; DMEM, Dulbecco's modified Eagle medium; FBS, fetal bovine serum; $NaHCO_3$, sodium bicarbonate; HBSS, Hanks' balanced salt solution; PCC, Pearson's correlation coefficient; $MgSO_4$, magnesium sulfate; $CHCl_3$, chloroform

■ REFERENCES

(1) Senapati, S.; Mahanta, A. K.; Kumar, S.; Maiti, P. Controlled drug delivery vehicles for cancer treatment and their performance. *Signal Transduction Targeted Ther.* **2018**, *3*, 7.

(2) Patra, J. K.; Das, G.; Fraceto, L. F.; Campos, E. V. R.; Rodriguez-Torres, M. d. P.; Acosta-Torres, L. S.; Diaz-Torres, L. A.; Grillo, R.; Swamy, M. K.; Sharma, S.; Habtemariam, S.; Shin, H.-S. Nano based drug delivery systems: recent developments and future prospects. *J. Nanobiotechnol.* **2018**, *16*, 71.

(3) (a) Park, S.; Kim, E.; Kim, W. Y.; Kang, C.; Kim, J. S. Biotin-guided anticancer drug delivery with acidity-triggered drug release. *Chem. Commun.* **2015**, *51*, 9343−9345. (b) Mao, J.; Li, Y.; Wu, T.; Yuan, C.; Zeng, B.; Xu, Y.; Dai, L. A simple dual-pH responsive prodrug-based polymeric micelles for drug delivery. *ACS Appl. Mater. Interfaces* **2016**, *8*, 17109−17117.

(4) (a) Zhao, J.; Hua, W.; Xu, G.; Gou, S. Biotinylated platinum(IV) complexes designed to target cancer cells. *J. Inorg. Biochem.* **2017**, *176*, 175−180. (b) Lee, M. H.; Sessler, J. L.; Kim, J. S. Disulfide-based multifunctional conjugates for targeted theranostic drug delivery. *Acc. Chem. Res.* **2015**, *48*, 2935−2946.

(5) Kim, E. J.; Bhuniya, S.; Lee, H.; Kim, H. M.; Cheong, C.; Maiti, S.; Hong, K. S.; Kim, J. S. An activatable prodrug for the treatment of metastatic tumors. *J. Am. Chem. Soc.* **2014**, *136*, 13888−13894.

(6) (a) Liu, P.; Xu, J.; Yan, D.; Zhang, P.; Zeng, F.; Li, B.; Wu, S. A DT-diaphorase responsive theranostic prodrug for diagnosis, drug release monitoring and therapy. *Chem. Commun.* **2015**, *51*, 9567−9570. (b) Shin, W. S.; Han, J.; Verwilst, P.; Kumar, R.; Kim, J.-H.; Kim, J. S. Cancer targeted enzymatic theranostic prodrug: precise diagnosis and chemotherapy. *Bioconjugate Chem.* **2016**, *27*, 1419−1426.

(7) (a) Chen, K. J.; Liang, H. F.; Chen, H. L.; Wang, Y. C.; Cheng, P. Y.; Liu, H. L.; Xia, Y. N.; Sung, H. W. A thermoresponsive bubble-generating liposomal system for triggering localized extracellular drug delivery. *ACS Nano* **2013**, *7*, 438−446. (b) Wang, D.; Huang, H.; Zhou, M.; Lu, H.; Chen, J.; Chang, Y. T.; Gao, J.; Chai, Z.; Hu, Y. A thermoresponsive nanocarrier for mitochondria-targeted drug delivery. *Chem. Commun.* **2019**, *55*, 4051−4054.

(8) (a) Klan, P.; Solomek, T.; Bochet, C. G.; Blanc, A.; Givens, R.; Rubina, M.; Popik, V.; Kostikov, A.; Wirz, J. Photoremovable protecting groups in chemistry and biology: reaction mechanisms and efficacy. *Chem. Rev.* **2013**, *113*, 119−191. (b) Shin, W. S.; Han, J.; Kumar, R.; Lee, G. G.; Sessler, J. L.; Kim, J.- H.; Kim, J. S. Programmed activation of cancer cell apoptosis: a tumor-targeted phototherapeutic topoisomerase I inhibitor. *Sci. Rep.* **2016**, *6*, 29018−29028. (c) Lin, Q.; Huang, Q.; Li, C.; Bao, C.; Liu, Z.; Li, F.; Zhu, L. Anticancer drug release from a mesoporous silica based nanophotocage regulated by either a one- or two-photon process. *J. Am. Chem. Soc.* **2010**, *132*, 10645−10647.

(9) (a) Olejniczak, J.; Carling, C.-J.; Almutairi, A. Photocontrolled release using one-photon absorption of visible or NIR light. *J. Controlled Release* **2015**, *219*, 18−30. (b) Linsley, C. S.; Wu, B. M. Recent advances in light-responsive on-demand drug-delivery systems. *Ther. Delivery* **2017**, *8*, 89−107.

(10) (a) Zhao, H.; Sterner, E. S.; Coughlin, E. B.; Theato, P. *O*-nitrobenzyl alcohol derivatives: Opportunities in polymer and materials science. *Macromolecules* **2012**, *45*, 1723−1736. (b) Shah, S.; Sasmal, P. K.; Lee, K. B. Photo-triggerable hydrogel−nanoparticle hybrid scaffolds for remotely controlled drug delivery. *J. Mater. Chem. B* **2014**, *2*, 7685−7693.

(11) (a) Furuta, T.; Wang, S. S.; Dantzker, J. L.; Dore, T. M.; Bybee, W. J.; Callaway, E. M.; Denk, W.; Tsien, R. Y. Brominated 7-hydroxycoumarin-4-ylmethyls: photolabile protecting groups with biologically useful cross-sections for two photon photolysis. *Proc. Natl. Acad. Sci. U. S. A.* **1999**, *96*, 1193−1200. (b) Liu, P.; Li, B.; Zhan, C.; Zeng, F.; Wu, S. A two-photon-activated prodrug for therapy and drug release monitoring. *J. Mater. Chem. B* **2017**, *5*, 7538−7546. (c) Ji, W.; Li, N.; Chen, D.; Qi, X.; Sha, W.; Jiao, Y.; Xu, Q.; Lu, J. Coumarin-containing photo-responsive nanocomposites for NIR light-triggered controlled drug release via a two-photon process. *J. Mater. Chem. B* **2013**, *1*, 5942−5949.

(12) Wells, L. A.; Brook, M. A.; Sheardown, H. Generic, Anthracene-based hydrogel crosslinkers for photo-controllable drug delivery. *Macromol. Biosci.* **2011**, *11*, 988−998.

(13) Asad, N.; Deodato, D.; Lan, X.; Widegren, M. B.; Phillips, D. L.; Du, L.; Dore, T. M. Photochemical activation of tertiary amines for applications in studying cell physiology. *J. Am. Chem. Soc.* **2017**, *139*, 12591−12600.

(14) (a) Houk, A. L.; Givens, R. S.; Elles, C. G. Two-photon activation of *p*-hydroxyphenacyl phototriggers: toward spatially controlled release of diethyl phosphate and ATP. *J. Phys. Chem. B* **2016**, *120*, 3178−3186. (b) Barman, S.; Mukhopadhyay, S. K.; Biswas, S.; Nandi, S.; Gangopadhyay, M.; Dey, S.; Anoop, A.; Singh, N. D. P. A *p*-hydroxyphenacyl-benzothiazole-chlorambucil conjugate as a real-time-monitoring drug-delivery system assisted by excited-state intramolecular proton transfer. *Angew. Chem., Int. Ed.* **2016**, *55*, 4194−4198. (c) Singh, A. K.; Kundu, M.; Roy, S.; Roy, B.; Shah, S. S.; Nair, A. V.; Pal, B.; Mondal, M.; Singh, N. D. P. A two-photon responsive naphthyl tagged *p*-hydroxyphenacyl based drug delivery system: uncaging of anti-cancer drug in the phototherapeutic window with real-time monitoring. *Chem. Commun.* **2020**, *56*, 9986−9989.

(15) (a) Turner, A. D.; Pizzo, S. V.; Rozakis, G. W.; Porter, N. A. Photochemical activation of acylated α-thrombin. *J. Am. Chem. Soc.* **1987**, *109*, 1274−1275. (b) Turner, A. D.; Pizzo, S. V.; Rozakis, G.; Porter, N. A. Photoreactivation of irreversibly inhibited serine proteinases. *J. Am. Chem. Soc.* **1988**, *110*, 244−250. (c) Gagey, N.; Neveu, P.; Jullien, L. Two-photon uncaging with the efficient 3,5-dibromo-2,4-dihydroxycinnamic caging group. *Angew. Chem., Int. Ed.*

https://doi.org/10.1021/acs.jmedchem.1c00956
J. Med. Chem. XXXX, XXX, XXX−XXX

2007, *46*, 2467−2469. (d) Gagey, N.; Neveu, P.; Benbrahim, C.; Goetz, B.; Aujard, I.; Baudin, J. B.; Jullien, L. Two-photon uncaging with fluorescence reporting: evaluation of the *o*-hydroxycinnamic platform. *J. Am. Chem. Soc.* **2007**, *129*, 9986−9998. (e) Duan, X.-Y.; Zhai, B.-C.; Song, Q.-H. Water-soluble *o*-hydroxycinnamate as an efficient photoremovable protecting group of alcohols with fluorescence reporting. *Photochem. Photobiol. Sci.* **2012**, *11*, 593−598. (f) Paul, A.; Mengji, R.; Chandy, O. A.; Nandi, S.; Bera, M.; Jana, A.; Anoop, A.; Singh, N. D. P. ESIPT-induced fluorescent *o*-hydroxycinnamate: a self-monitoring phototrigger for prompt image-guided uncaging of alcohols. *Org. Biomol. Chem.* **2017**, *15*, 8544−8552. (g) Venkatesh, Y.; Srivastava, H. K.; Bhattacharya, S.; Mehra, M.; Datta, P. K.; Bandyopadhyay, S.; Singh, N. D. P. One- and two-photon uncaging: carbazole fused *o*-hydroxycinnamate platform for dual release of alcohols (same or different) with real-time monitoring. *Org. Lett.* **2018**, *20*, 2241−2244. (h) Paul, A.; Bera, M.; Gupta, P.; Singh, N. D. P. *o*-Hydroxycinnamate for sequential photouncaging of two different functional groups and its application in releasing cosmeceuticals. *Org. Biomol. Chem.* **2019**, *17*, 7689−7693.

(16) Feng, W.; Gao, C.; Liu, W.; Ren, H.; Wang, C.; Ge, K.; Li, S.; Zhou, G.; Li, H.; Wang, S.; Jia, G.; Li, Z.; Zhang, J. A novel anticancer theranostic pro-prodrug based on hypoxia and photo sequential control. *Chem. Commun.* **2016**, *52*, 9434−9437.

(17) (a) Murphy, M. P.; Smith, R. A. Drug delivery to mitochondria: the key to mitochondrial medicine. *Adv. Drug Delivery Rev.* **2000**, *41*, 235−250. (b) Wang, P.; Song, J. H.; Song, D. K.; Zhang, J.; Hao, C. Role of death receptor and mitochondrial pathways in conventional chemotherapy drug induction of apoptosis. *Cell. Signalling* **2006**, *18*, 1528−1535.

(18) Yue, C.; Yang, Y.; Song, J.; Alfranca, G.; Zhang, C.; Zhang, Q.; Yin, T.; Pan, F.; de la Fuente, J. M.; Cui, D. Mitochondria-targeting near-infrared light-triggered thermosensitive liposomes for localized photothermal and photodynamic ablation of tumors combined with chemotherapy. *Nanoscale* **2017**, *9*, 11103−11118.

(19) Ju, E.; Li, Z.; Liu, Z.; Ren, J.; Qu, X. Near-infrared light-triggered drug-delivery vehicle for mitochondria-targeted chemo-photothermal therapy. *ACS Appl. Mater. Interfaces* **2014**, *6*, 4364−4370.

(20) Marrache, S.; Tundup, S.; Harn, D. A.; Dhar, S. *Ex vivo* programming of dendritic cells by mitochondria-targeted nanoparticles to produce interferon-gamma for cancer immunotherapy. *ACS Nano* **2013**, *7*, 7392−7402.

(21) Paul, A.; Mengji, R.; Bera, M.; Ojha, M.; Jana, A.; Singh, N. D. P. Mitochondria-localized in situ generation of rhodamine photocage with fluorescence turn-on enabling cancer cell-specific drug delivery triggered by green light. *Chem. Commun.* **2020**, *56*, 8412−8415.

(22) Dabrowski, J. M.; Arnaut, L. G. Photodynamic therapy (PDT) of cancer: from local to systemic treatment. *Photochem. Photobiol. Sci.* **2015**, *14*, 1765−1780.

(23) (a) Smith, R. A.; Porteous, C. M.; Gane, A. M.; Murphy, M. P. Delivery of bioactive molecules to mitochondria. *Proc. Natl. Acad. Sci. U. S. A.* **2003**, *100*, 5407−5412. (b) Liu, H.-N.; Guo, N.-N.; Wang, T.-T.; Guo, W.-W.; Lin, M.-T.; Huang-Fu, M.-Y.; Vakili, M. R.; Xu, W.-H.; Chen, J.-J.; Wei, Q.-C.; Han, M.; Lavasanifar, A.; Gao, J.-Q. Mitochondrial targeted doxorubicin-triphenylphosphonium delivered by hyaluronic acid modified and pH responsive nanocarriers to breast tumor: *in vitro* and *in vivo* studies. *Mol. Pharmaceutics* **2018**, *15*, 882−891.

(24) Zhang, R.; Qin, X.; Kong, F.; Chen, P.; Pan, G. Improving cellular uptake of therapeutic entities through interaction with components of cell membrane. *Drug Delivery* **2019**, *26*, 328−342.

(25) Gupta, A.; Prasad, P.; Gupta, S.; Sasmal, P. K. Simultaneous ultrasensitive detection and elimination of drug-resistant bacteria by cyclometalated iridium(III) complexes. *ACS Appl. Mater. Interfaces* **2020**, *12*, 35967−35976.

(26) Ash, C.; Dubec, M.; Donne, K.; Bashford, T. Effect of wavelength and beam width on penetration in light-tissue interaction using computational methods. *Lasers Med. Sci.* **2017**, *32*, 1909−1918.

https://doi.org/10.1021/acs.jmedchem.1c00956
J. Med. Chem. XXXX, XXX, XXX−XXX